# Individual switching of film-based nanoscale epitaxial ferroelectric capacitors

Yunseok Kim,[1,a)] Hee Han,[2] Brian J. Rodriguez,[1,b)] Ionela Vrejoiu,[1] Woo Lee,[3] Sunggi Baik,[2] Dietrich Hesse,[1] and Marin Alexe[1]
[1]*Max Planck Institute of Microstructure Physics, D-06120 Halle (Saale), Germany*
[2]*Department of Materials Science and Engineering, Pohang University of Science and Technology (POSTECH), Pohang 790-784, Republic of Korea*
[3]*Korea Research Institute of Standards and Science (KRISS), Yuseong, 305-340 Daejeon, Republic of Korea*

(Received 5 October 2009; accepted 22 April 2010; published online 31 August 2010)

We have investigated the individual switching of nanoscale capacitors by piezoresponse force microscopy. Nanoscale epitaxial ferroelectric capacitors with terabyte per inch square equivalent density were fabricated by the deposition of top electrodes onto a pulsed laser deposited lead zirconate titanate thin film by electron beam evaporation through ultrathin anodic aluminum oxide membrane stencil masks. Using bias pulses, the nanoscale capacitors were uniformly switched and proved to be individually addressable. These film-based nanoscale capacitors might be a feasible alternative for high-density mass storage memory applications with near terabyte per inch square density due to the absence of any cross-talk effects. © *2010 American Institute of Physics*. [doi:10.1063/1.3474960]

## I. INTRODUCTION

Among various nonvolatile memory devices, ferroelectric memories are still investigated due to their unique advantages such as high density, low power consumption, and high read/write speed.[1–3] As there is an increasing demand for a very high memory density near terabyte per inch square, the size of ferroelectric capacitors needs to be scaled down to the nanoscale range while avoiding detrimental size-effects. There have been many efforts to fabricate and analyze individually addressable nanoscale ferroelectric capacitors.[4–12] Several different fabrication methods such as chemical solution deposition, focused ion-beam (FIB), and *e*-beam lithography have been used for ferroelectric nanostructure fabrication.[6–15] FIB has been almost exclusively used to fabricate ferroelectric capacitors. However, the area near the surface can be damaged during processing.[9–11] As the capacitor size becomes very small, close to the nanoscale range, the beam damage may have a serious detrimental influence on the ferroelectric properties of the capacitor. Recently we reported an anodic aluminum oxide (AAO)-based fabrication method which can be easily applied to fabricate nanoscale ferroelectric capacitors and structures without any significant detrimental effects.[6,8] This AAO-based fabrication method is a unique approach for the high quality fabrication of nanostructures and the subsequent solvent-free lift-off process is suitable for even very sensitive materials.[6] Therefore, this approach may give us reliable access to smaller capacitors than conventional approaches such as FIB or *e*-beam lithography.

The AAO-based fabrication method allows the fabrication of different types of structures such as metal island/ferroelectric island/metal film (MIFI), metal island/ferroelectric film/metal film (MIFF), and ferroelectric island/metal film (FI).[5–8] Among them, we recently reported the use of the AAO-based method for the fabrication of MIFI and FI nanostructures.[6,7] It was found that the individual nanoscale capacitors in these structures are physically separated, and thus the electric field can be effectively concentrated. In addition, each nanoscale capacitor exhibits significantly improved piezoresponse compared to the film-based counterparts as a result of the strain relief that is associated with the crystal structure.[6] However, by further decreasing the size of the nanoscale capacitors, the ferroelectric properties and the crystallization of nanoscale islands are expected to become difficult to control compared to the case of MIFF, where scaling-down of the top metal electrodes on an epitaxially grown ferroelectric film is much more amenable.

In this study, we show the preparation of film-based nanoscale ferroelectric capacitors (MIFF structures) on epitaxial lead zirconate titanate (PZT) thin films using an AAO-based fabrication procedure. Switching behavior, including cross-talk, of individual nanoscale capacitors has been studied using piezoresponse force microscopy (PFM).

## II. EXPERIMENT

An epitaxial $Pb(Zr_{0.2}Ti_{0.8})O_3$ (PZT20/80) thin film with a thickness of 35 nm was deposited at 650 °C under 100 mTorr oxygen by pulsed laser deposition (PLD) of a KrF excimer laser with a wavelength of 248 nm, an energy fluence of 500 $mJcm^{-2}$, and a repetition rate of 5–10 Hz on an (001) oriented 150 nm thick Pt bottom electrode on an MgO substrate. Self-ordered ultrathin AAO masks were prepared by anodization of aluminum[6,7] and placed on the PZT/Pt/MgO substrate, as shown in Fig. 1. 15 nm thick Pt was subsequently deposited by electron beam evaporation. Finally, the Pt/PZT/Pt nanoscale capacitors were obtained by removing the AAO mask. The sizes of nanoscale capacitors

[a)]Electronic mail: ykim@mpi-halle.mpg.de.
[b)]Present address: University College Dublin, Belfield, Dublin 4, Ireland.

 

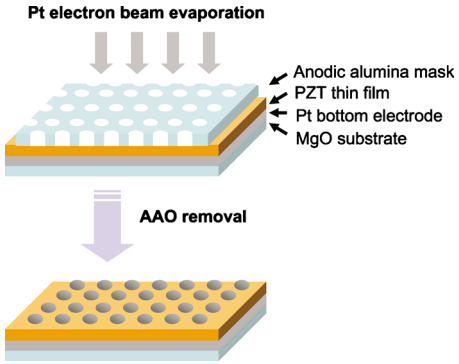


FIG. 1. (Color online) Schematic of the fabrication procedure for nanoscale epitaxial ferroelectric capacitors.

can be easily tuned by controlling the pore radius of the AAO mask, which depends on the electrochemical parameters of anodization. Micron-scale capacitors were fabricated using an 150 nm thick epitaxial PZT20/80 tetragonal c-axis oriented thin film deposited on $SrRuO_3/SrTiO_3(001)$ by PLD as described elsewhere.[16] 50 nm thick Pt top electrodes of $1.5\times1.5$ $\mu m^2$ were sputtered and patterned by electron beam lithography and lift-off.

PFM measurements were performed under ambient conditions using commercial atomic force microscopes (AFM-XE-100, Park Systems and AutoProbe CP Research, TM Microscopes) with lock-in amplifier (SR830, Stanford Research Systems). The PFM measurement is based on the detection of the local electromechanical vibration of the ferroelectric materials caused by an external ac voltage, and it has been widely used for the investigation of ferroelectric nanostructures due to its high spatial resolution, easy implementation, and effective polarization manipulation capabilities.[17,18] To obtain local piezoresponse images and hysteresis loops, an ac modulation voltage of 0.2 $V_{rms}$ at 6.5–25 kHz was applied to the $PtIr_5$-coated silicon cantilevers (ATEC-EFM, Nanosensors) with a spring constant of 2.8 N/m and a resonance frequency of 75 kHz. The local piezoresponse hysteresis

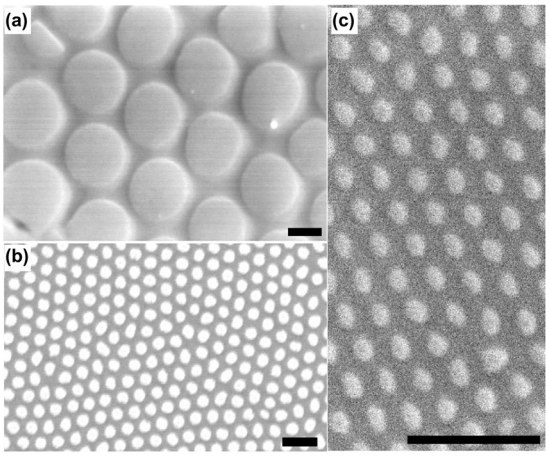


FIG. 2. SEM images of nanoscale epitaxial ferroelectric capacitors with different radius: (a) 190 nm, (b) 35 nm, and (c) 20 nm, respectively. (c) shows a deposited nanoscale capacitor array with the AAO mask (bottom) and its magnified view (top). (Scale bars are 200 nm.)

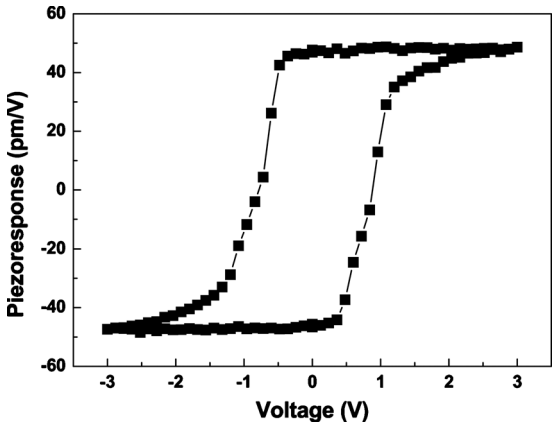


FIG. 3. Piezoresponse hysteresis loop of a nanoscale epitaxial ferroelectric capacitor with a radius of 35 nm.

loops were measured by applying bias voltages from −3 to +3 V for more than 100 nanoscale capacitors.

## III. RESULTS AND DISCUSSION

Figure 2 shows MIFF structures with different radii fabricated by the AAO-based method shown in Fig. 1. To fabricate nanoscale capacitors of different sizes, the pore radius of the AAO mask was controlled by different electrolyte and anodization voltages.[19] The average radius of the final capacitor is roughly the same as the pore radius of the used AAO mask. As shown in Fig. 2, all nanoscale capacitors are well ordered and the smallest nanoscale capacitors in Fig. 2(c) yield a capacitor density of about 1 Tb $in.^{-2}$.

The piezoresponse hysteresis loop of the nanoscale capacitors with a radius of 35 nm is presented in Fig. 3. The rectangular shape of the hysteresis loop indicates the high quality of the present epitaxial PZT thin film. The positive and the negative remnant piezoelectric coefficient $(R_0)$ [coercive voltages $(V_C)$] are $47.3\pm5.3$ pm/V $[0.81\pm0.21$ V] and $-46.4\pm5.5$ pm/V $[-0.82\pm0.25$ V], respectively. The histograms of each value can be found in Fig. 4. Especially, the histogram of the remnant polarization shows very uniform piezoresponse on each of the nanoscale capacitors. The nanoscale capacitors have an average coercive voltage of

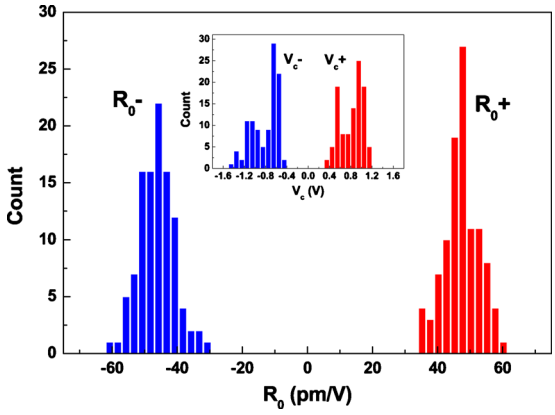


FIG. 4. (Color online) Histogram of the positive and the negative remnant piezoelectric coefficient distributions for more than 100 nanoscale capacitors with a radius of 35 nm. The inset presents the histogram of the positive and the negative coercive voltage distributions.

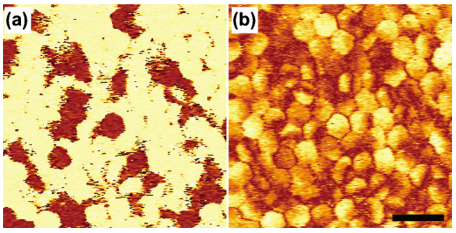


FIG. 5. (Color online) (a) Phase and (b) amplitude PFM images of as-deposited capacitors with a radius of 35 nm. (Scale bar is 200 nm.)

about 0.82 V and an average effective remnant piezoelectric coefficient of about 46.9 pm/V. The piezoelectric coefficient is smaller compared to that of a MIFI structure fabricated in a similar way due to mechanical constrains in the thin film.[4,6]

Figure 5 shows PFM phase and amplitude images of the as-deposited nanoscale capacitors with a radius of 35 nm showing uniform PFM response of well-ordered capacitors. Upward polarized regions are randomly distributed in the as-deposited capacitors. The domains observed through the Pt top electrodes do not appear to be affected by the fabrication process and may directly follow the as-deposited domains of the epitaxial PZT thin film. Some capacitors showed single domain structures, while others consisted of domains. After application of a bias pulse, however, the as-deposited domain structure can be manipulated.

Figure 6 shows a typical individual switching experiment. A collection of capacitors were switched downwards by applying a negative bias. Then, the polarization of a selected capacitor was switched upward by applying a positive bias pulse. Only the target capacitor was switched in the desired direction without any influence on the surrounding capacitors. As we noticed in the as-fabricated state (Fig. 5) the ferroelectric domains can extend through several capacitors. However, when the bias pulses are applied to the individual capacitors, the newly formed domain is confined by the boundaries of the capacitor. Theoretical analysis of the electric field distribution at the nanoscale capacitors showed that the electric field can propagate toward the outside of the capacitors.[6,20] These fringing fields can push the domains outside of the capacitor, generating a significant cross-talk.[21,22] However, our experimental results show that the newly formed domain is completely confined by the capacitor boundaries and no cross-talk occurs during the polarization switching.

For comparison, micron-scale capacitors were fabricated by electron beam lithography and lift-off on top of the 150 nm PZT film grown on $SrRuO_3/SrTiO_3(001)$. As presented

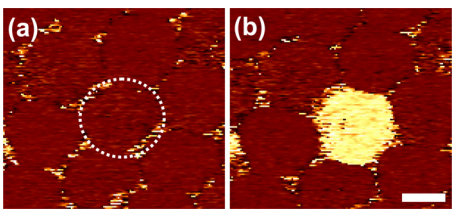


FIG. 6. (Color online) PFM phase images of (a) a background poled and (b) a back-switched nanoscale capacitor. Scale bar is 50 nm. The dashed line in (a) indicates the location of the capacitor.

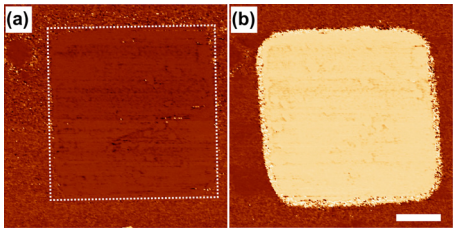


FIG. 7. (Color online) PFM phase images of (a) a background poled and (b) a back-switched micron-scale capacitor. (Scale bar is 360 nm.) The dashed line in (b) indicates the location of the capacitor.

in Fig. 7, a microscale capacitor was switched in desired tetragonal c-axis orientation and as expected the switched region was confined within the capacitor. For both signs of applied bias pulses, the domains in Fig. 7 were clearly confined by the capacitor boundaries and this confinement at the boundary was reproducible. However, further investigation will be conducted to clarify the influence of the aspect ratio on the domain confinement.

The present observations clearly reveal that the fringing fields do not represent a critical limitation for both nanoscale and microscale capacitors, provided that the aspect ratio (i.e., the ratio of the lateral size to the thickness) of the capacitor is larger than one, for which condition a unidirectional distribution of the electric field can be effectively achieved from the top to the bottom of the PZT film.

Although the present film-based capacitors have many attractive points for memory devices, there is also limitation for their application. As previously mentioned, the piezoelectric coefficient of MIFF structures is much smaller than that of MIFI structures.[4,6] In order to decrease the size of the capacitor, the film thickness must also be reduced in order to keep the aspect ratio and preserve the domain stability.[23] Decreasing the thickness of ferroelectric thin films could result in detrimental size-effects.[24] Thus, for continued miniaturization of capacitors, high quality epitaxial films should be used. Furthermore, control of extended structural defects, such as misfit and/or threading dislocations, might be crucial in achieving uniform ferroelectric and piezoelectric properties.

## IV. SUMMARY

In summary, we have fabricated arrays of nanoscale epitaxial ferroelectric capacitors with metal island/ferroelectric film/metal film (MIFF) configuration, and investigated the switching behavior of individual nanoscale capacitors. Using ultrathin AAO membrane stencil masks, and by taking advantage of the unique tailoring capability of their pore sizes, different sizes of film-based nanoscale ferroelectric capacitors could be fabricated on epitaxial PZT thin films. The memory density of arrays of nanoscale capacitors with the smallest radius (20 nm) and separation (60 nm) corresponds to almost 1 Tb $in.^{-2}$. The switching of a single capacitor proceeds in the form of a single domain, which in any case is confined by the capacitor boundaries. Thus there is no cross-talk between adjacent capacitors. These film-based nanoscale

capacitors might be a feasible alternative for high-density mass storage memory applications with near terabyte per inch square density.

## ACKNOWLEDGMENTS

We acknowledge the financial support of the Alexander von Humboldt Foundation (Y.K. and B.J.R.) and the support in part from KRCF through the project "Development of Advanced Industrial Metrology," as well as by a joint effort of the German Science Foundation (DFG) and the Korean Research Foundation within a DFG-KRF project (446 KOR 113/215).

[1]J. F. Scott and C. A. Paz de Araujo, Science **246**, 1400 (1989).
[2]O. Auciello, J. F. Scott, and R. Ramesh, Phys. Today **51**(7), 22 (1998).
[3]J. F. Scott, Science **315**, 954 (2007).
[4]V. Nagarajan, A. Roytburd, A. Stanishevsky, S. Prasertchoung, T. Zhao, L. Chen, J. Melngailis, O. Auciello, and R. Ramesh, Nature Mater. **2**, 43 (2003).
[5]A. Gruverman, D. Wu, and J. F. Scott, Phys. Rev. Lett. **100**, 097601 (2008).
[6]W. Lee, H. Han, A. Lotnyk, M. A. Schubert, S. Senz, M. Alexe, D. Hesse, S. Baik, and U. Gösele, Nat. Nanotechnol. **3**, 402 (2008).
[7]B. J. Rodriguez, X. S. Gao, L. F. Liu, W. Lee, I. I. Naumov, A. M. Bratkovsky, D. Hesse, and M. Alexe, Nano Lett. **9**, 1127 (2009).
[8]H. Han, K. Lee, W. Lee, M. Alexe, D. Hesse, and S. Baik, J. Mater. Sci. **44**, 5167 (2009).
[9]M. Alexe, C. Harnagea, D. Hesse, and U. Gösele, Appl. Phys. Lett. **75**, 1793 (1999).
[10]A. Stanishevsky, B. Nagaraj, J. Melngailis, R. Ramesh, L. Khriachtchev, and E. McDaniel, J. Appl. Phys. **92**, 3275 (2002).
[11]M. Alexe, C. Harnagea, and D. Hesse, J. Electroceram. **12**, 69 (2004).
[12]T. Sun, Z. Pan, V. P. Dravid, Z. Wang, M.-F. Yu, and J. Wang, Appl. Phys. Lett. **89**, 163117 (2006).
[13]S. Bühlmann, P. Muralt, and S. Von Allmen, Appl. Phys. Lett. **84**, 2614 (2004).
[14]H. Han, R. Ji, Y. J. Park, S. K. Lee, G. Le Rhun, M. Alexe, K. Nielsch, D. Hesse, U. Gösele, and S. Baik, Nanotechnology **20**, 015301 (2009).
[15]S. Clemens, S. Röhrig, A. Rüdiger, T. Schneller, and R. Waser, Nanotechnology **20**, 075305 (2009).
[16]I. Vrejoiu, G. Le Rhun, L. Pintilie, D. Hesse, M. Alexe, and U. Gösele, Adv. Mater. **18**, 1657 (2006).
[17]S. V. Kalinin, S. Jesse, B. J. Rodriguez, K. Seal, A. P. Baddorf, T. Zhao, Y. H. Chu, R. Ramesh, E. A. Eliseev, A. N. Morozovska, B. Mirman, and E. Karapetian, Jpn. J. Appl. Phys., Part 1 **46**, 5674 (2007).
[18]N. Balke, I. Bdikin, S. V. Kalinin, and A. Kholkin, J. Am. Ceram. Soc. **92**, 1629 (2009).
[19]A. P. Li, F. Müller, A. Birner, K. Nielsch, and U. Gösele, J. Appl. Phys. **84**, 6023 (1998).
[20]P. R. Evans, X. H. Zhu, P. Baxter, M. McMillen, J. McPhillips, F. D. Morrison, J. F. Scott, R. J. Pollard, R. M. Bowman, and J. M. Gregg, Nano Lett. **7**, 1134 (2007).
[21]J.-Z. Bao and C. C. Davis, Phys. Rev. E **47**, 3670 (1993).
[22]N. Ng, R. Ahluwalia, H. B. Su, and F. Boey, Acta Mater. **57**, 2047 (2009).
[23]J. Woo, S. Hong, D. K. Min, H. Shin, and K. No, Appl. Phys. Lett. **80**, 4000 (2002).
[24]A. N. Morozovska, S. V. Svechnikov, E. A. Eliseev, and S. V. Kalinin, Phys. Rev. B **76**, 054123 (2007).